Absorption Spectra of Photoactive Yellow Protein Chromophores in Vacuum

I. B. Nielsen,* S. Boyé-Péronne,† M. O. A. El Ghazaly,* M. B. Kristensen,* S. Brøndsted Nielsen,* and L. H. Andersen*

*Department of Physics and Astronomy, University of Aarhus, Aarhus, Denmark; and †Laboratoire de Photophysique Moléculaire, Paris-Sud University, Orsay Cédex, France

ABSTRACT The absorption spectra of two photoactive yellow protein model chromophores have been measured in vacuum using an electrostatic ion storage ring. The absorption spectrum of the isolated chromophore is an important reference for deducing the influence of the protein environment on the electronic energy levels of the chromophore and separating the intrinsic properties of the chromophore from properties induced by the protein environment. In vacuum the deprotonated *trans*-thiophenyl-*p*-coumarate model chromophore has an absorption maximum at 460 nm, whereas the photoactive yellow protein absorbs maximally at 446 nm. The protein environment thus only slightly blue-shifts the absorption. In contrast, the absorption of the model chromophore in aqueous solution is significantly blue-shifted ($\lambda_{max} = 395$ nm). A deprotonated *trans-p*-coumaric acid has also been studied to elucidate the effect of thioester formation and phenol deprotonation. The sum of these two changes on the chromophore induces a red shift both in vacuum and in aqueous solution.

INTRODUCTION

The photoactive yellow protein (PYP) functions as a blue light sensor in certain bacteria. Absorption of blue light by the protein results in a signal being generated and transmitted to the bacterium. In this way the bacterium can move away from the possibly damaging blue light (1). Being a photosensor, PYP belongs to the group of photoactive proteins including the rhodopsins, the phytochromes, and the cryptochromes (2). The common theme is that light absorption in the chromophore triggers a photocycle in the protein. First, conformational changes involving only the chromophore atoms are taking place, for example, a *trans*/*cis* isomerization. The changes in the chromophore structure are then followed by larger conformational changes of the overall protein structure, which ultimately lead to the biological response (2).

PYP is a rather small water-soluble protein with 125 amino acids, and it has a bright yellow color due to its absorption of blue light, with a maximum absorption at 446 nm (3). The protein was first discovered in the purple halophilic bacterium *Halorhodospira halophila*, also known as *Ectothiorhodospira halophila*. The bacterium is phototrophic, meaning that it needs the energy from light to perform essential processes, and therefore it moves toward areas with light. However, it also shows a negative response toward blue light, probably to avoid photodamage. Since the action spectrum for this negative phototaxis almost exactly matches the absorption spectrum of PYP, it seems likely that PYP serves as the photosensor for this response (1).

The chromophore responsible for light absorption in PYP is a *p*-coumaric acid (see Fig. 1 *A*). In the ground state the chromophore is in the *trans* form, the phenol group is deprotonated (4,5), and it is covalently linked to the protein via a thioester linkage to cysteine residue 69. It is the highly conjugated nature of the chromophore that provides absorption in the visible region. Upon absorption of a blue photon, PYP enters a photocycle that has been studied in great detail (6–13). During the 1-s photocycle the chromophore isomerizes to the *cis* form, the phenolate is protonated from a nearby glutamic acid (Glu-46), and large conformational changes of the protein take place. These changes result in generation of a signal to the bacterium before the protein returns to the ground state.

The ground-state secondary structure of PYP is an α/β-fold with a central β-sheet surrounded by several α-helices (14). There are two hydrophobic pockets in the structure, and the chromophore is situated in the main pocket. A hydrogen-bonding network with the nearby amino acids Glu-46, Tyr-42, and Thr-50 stabilizes the negative charge on the chromophore, which is further stabilized by delocalization of the negative charge over the conjugated area. Possibly the positive charge on the nearby Arg-52 residue also has an effect in stabilizing the negative charge as well as shielding the chromophore from the solvent in the ground state.

Since light is absorbed by the chromophore and the first reactions in the photocycle take place here, the intrinsic properties of the chromophore are of immediate interest. These are determined by the charge state, the electron delocalization, and the substituents attached to the conjugated system. But it is also well known that the environment surrounding the chromophore is important for tuning the absorption maximum and guiding the chemical processes that occur during the photocycle. For the chromophore in the

Submitted February 25, 2005, and accepted for publication June 17, 2005.

Address reprint requests to L. H. Andersen, Dept. of Physics and Astronomy, University of Aarhus, DK-8000 Aarhus C, Denmark. Tel.: +45 89423605; Fax: +45 86120740; E-mail: lha@phys.au.dk.

0006-3495/05/10/2597/08 $2.00

doi: 10.1529/biophysj.105.061192

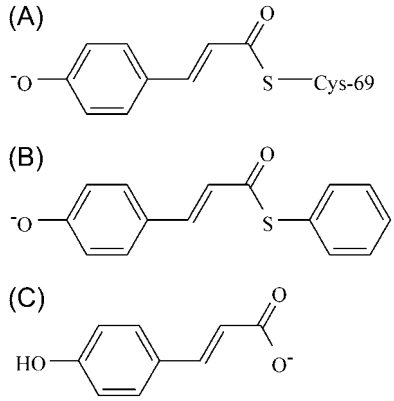

FIGURE 1 Structures of (*A*) the chromophore in PYP linked to Cys-69 together with the two model chromophores, (*B*) deprotonated *trans*-thiophenyl-*p*-coumarate (pCT^-), and (*C*) deprotonated *trans-p*-coumaric acid (pCA^-).

PYP protein this environment consists of the amino acids that reside close to or in the hydrophobic pocket where the chromophore is buried.

For years it has been a goal to try to separate the intrinsic properties of the chromophore from the role played by the protein environment. For this purpose, models of the chromophore have previously been studied in aqueous solutions using time-resolved spectroscopy methods to elucidate the dynamics after photon absorption (15–18), as well as in the gas phase as a neutral species to study the nature of the electronic states (19). Regarding the perturbations of the electronic states by the environment, proteins with mutations near the chromophore have been studied (20–25). Finally the chromophore has also been studied theoretically, both as an isolated species and in a model protein environment (26–29).

Our approach is to investigate the effect of the protein environment on the electronic states and separate this from the intrinsic properties of the chromophore by studying models of the chromophore in vacuum. In this way we achieve an important reference point for comparison to the absorption in other media and to calculations. Furthermore, data obtained in the gas phase are needed, as extrapolations based on solution phase data concerning the absorption maximum are nontrivial (30).

EXPERIMENTAL

Chromophore models

As chromophore models we use the deprotonated *trans*-thiophenyl-*p*-coumarate (pCT^-) and the deprotonated *trans-p*-coumaric acid (pCA^-) seen in Fig. 1, *B* and *C*, respectively. The pCT^- chromophore is probably a good model for the protein chromophore (Fig. 1 *A*) since the negative charge delocalization does not extend beyond the sulfur atom, as confirmed by calculations (28). In pCA the carboxylic acid hydrogen is more acidic than the phenol hydrogen, so the chromophore is probably deprotonated yielding the carboxylate rather than the phenolate. Hence, by also studying pCA^-, we may determine the effects on the absorption maximum of attaching the thioester group and deprotonating the phenol. To separate these two effects the absorption spectrum of the doubly deprotonated *trans-p*-coumaric acid should be measured. It was, however, not possible to produce a substantial ion beam of the doubly deprotonated species.

Solution spectra

Absorption spectra of model chromophores in aqueous solution are recorded by a UV/Vis spectrophotometer (ThermoSpectronic. Heλios α). For pCA, a spectrum is also recorded in H_2O with NaOH added (pH >11) to produce the doubly deprotonated chromophore. Likewise a spectrum is recorded for pCT^-. To avoid hydrolysis of the thioester group the pCT chromophore is dissolved in a borate(III)-buffer at pH 10.2 (16) instead of adding NaOH to the aqueous solution.

Gas phase spectra

To measure the absorption spectra of the model chromophores, gas-phase anions are stored in an electrostatic ion-storage ring (ELISA (31,32)), shown in Fig. 2. We irradiate the ions with a laser pulse of tunable wavelength, and the ions that absorb a photon increase their internal energy accordingly. Due to the increased energy the ions eventually break apart creating fragments, of which some are neutral. (For a discussion of the temperature of small systems and the decay of hot ions see Andersen et al. (33,34). By recording the yield of neutral fragments as a function of the wavelength we get the relative absorption cross section.

The gas-phase ions are produced in an electrospray ion source (35). The model chromophore is dissolved in a methanol solution, where, in the case of pCT, ammonia is added to produce deprotonated ions. The solution is pumped through a fused silica capillary to a stainless-steel needle with a bias voltage of $\sim$3 kV. From the needle the solution is electrosprayed toward the entrance of the ion source.

In the ion source the ions are first swept through a heated capillary where the solvent is evaporated, and the ions go into the gas phase. The ions are then steered through the ion source to a cylindrical ion trap where they accumulate. In the trap, helium is used as a buffer gas to cool the ions. After 100 ms accumulation time the ions are extracted as a bunch containing $\sim 10^4$ ions. The ion bunch is then accelerated to 22 kV and mass-to-charge selected by a bending magnet. The masses are 163 amu for pCA^- and 255 amu for pCT^-. Finally, after mass selection the ion bunch is injected into the storage ring, where it circulates with a revolution time of 50–60 μs.

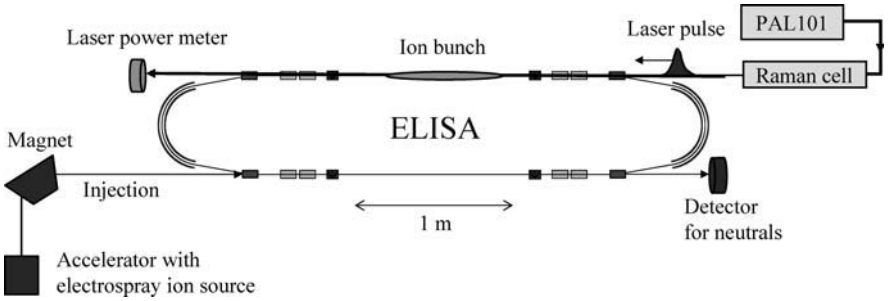

FIGURE 2 Electrostatic ion storage ring ELISA. The lower part of the ring is the injection and detection side, and the upper part is the laser interaction side. To the left is the electrospray ion source and the magnet for mass selection. The laser and the Raman cell are seen to the right.

At the end of one of the straight sections of ELISA a microchannel plate detector is situated (see Fig. 2). If ions in this section fragment by means of a collision or by photon absorption (see below), neutral fragments are formed and continue on straight trajectories to the detector. Hence, only neutral fragments produced in the injection section of the ring are detected. The counts from the detector are accumulated in a data-acquisition program in channels corresponding to the time after injection, so the time evolution of neutral production can be followed (see Fig. 3).

Before the interaction with the laser beam the ions are stored to allow decay of metastable ions formed in collisions during extraction from the trap. After 10–20 ms of storage there is only a background left of neutral counts from collisions with residual gas in the ring ($p \sim 10^{-11}$ mbar). A tunable nanosecond laser pulse is fired along the straight section opposite the injection side after ~60 ms of storage at a repetition rate of 10 Hz (see Fig. 2). The exact time of laser firing is adjusted to ensure maximum overlap with the ion bunch. Photon absorption will then either promptly or after some delay result in a breakup of the ions, thus creating neutral fragments that are detected if the dissociation takes place in the injection section.

To cover the desired wavelength range a pulsed Alexandrite laser (PAL101, Light Age, Somerset, NJ) in combination with a Raman cell is used. The Alexandrite laser is tunable in the range 720–800 nm. After the cavity the wavelength is frequency-doubled in a nonlinear crystal. The second harmonic is either used as it is or sent into a Raman cell with H_2 (360 psi) or D_2 (250 psi) from where the first and second Stokes lines are used. This provides wavelengths <399 nm (second harmonic), 413–443 nm (first Stokes in D_2), 428–470 nm (first Stokes in H_2), and 475–505 nm (second Stokes in D_2). After interaction with the ion bunch the laser pulse leaves the ring through a window, and the pulse energy is measured with a power meter. Typically the laser-pulse energy is kept around 0.2 mJ at 10 Hz. The laser-pulse energy is averaged over the data-acquisition time, which is 300 s, corresponding to 3000 injections.

Data analysis

Data sets with the number of counts from the microchannel plate detector as a function of time for the two chromophore models are shown in Fig. 3. The decay of hot ions immediately after injection, as well as the laser-induced signal, are clearly seen. It should be noted that the data shown here are taken with higher laser power than what is used to measure the absorption spectra.

There is an obvious difference between the signals for the two chromophores. For pCA^- (Fig. 3 *A*) there is a large increase in the number of neutral fragments after laser interaction. This continues over several revolutions in the storage ring. For pCT^-, on the other hand, we observe one peak with increased neutral production followed by a large depletion of the neutral signal (Fig. 3 *B*). The depletion shows that pCT^- has an unusually high-absorption cross section, and the single absorption peak shows that it decays with a time constant <~30 μs. Because of the fast decay only a small fraction of the photoexcited ions reach the

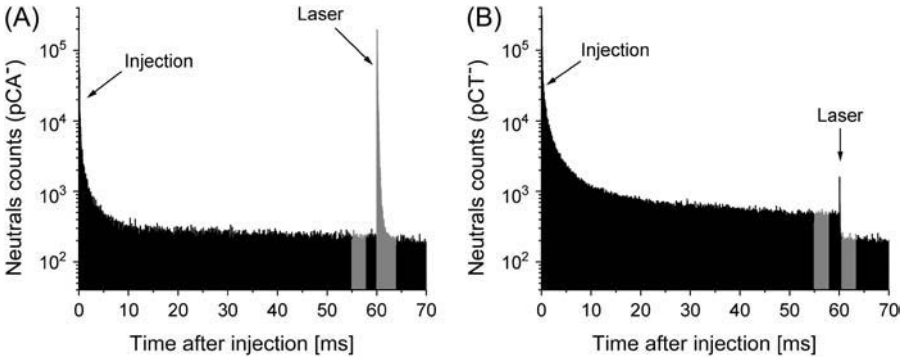

FIGURE 3 Number of neutral counts as a function of time is shown for the two model chromophores pCA^- (*A*) and pCT^- (*B*). The shaded areas show the time windows that give the integrated signal and background counts used in the calculation of the absorption cross section. Note that in 10 ms, there are 150–200 revolutions of the ion bunch.

opposite straight section before dissociation, and hence possibility of detection. A possible explanation for the fast decay could be that most of the ions decay via detachment of an electron. Direct photodetachment is ruled out since the cross section vanishes at high photon energies. The excited state that is reached by photoexcitation may, however, cause the resonance structure due to its coupling to the continuum.

Due to the different nature of the decay of the two photoexcited chromophores, two different yields are defined. For pCA^- the counts are integrated from the time of laser interaction to the time where the neutral count rate is reduced to the background level, giving $N_{signal}(\lambda)$ (second shaded window in Fig. 3 *A*). The average number of background counts (N_0) is determined by integrating the counts in a time window before the laser interaction, but after an almost stable background rate is reached (first shaded window in Fig. 3 *A*). Besides subtracting the background from the signal, the average background is also used as a measure of the number of ions in the storage ring. It can thus be used to normalize the signal, and the resulting fraction is termed the yield, $Y_{pCA^-}(\lambda)$, where λ is the wavelength of the laser light:

$$Y_{pCA^-}(\lambda) = \frac{N_{signal}(\lambda) - N_0}{N_0}. \quad (1)$$

For the pCT^- chromophore the depletion of the ion beam is used to obtain the yield. The integrated number of counts in a time window before and after the laser interaction (see Fig. 3 *B*) is used as a measure of the number of ions in the ring before (N_0), and after ($N(\lambda)$) laser interaction, respectively. The small peak, right after laser interaction, containing the neutral products from the ions surviving the first half round is not taken into consideration. The difference between the number of ions before and after laser interaction divided by N_0 gives the fraction of the ions in a bunch that have fragmented, and the yield is defined accordingly:

$$Y_{pCT^-}(\lambda) = \frac{N_0 - N(\lambda)}{N_0}. \quad (2)$$

For both chromophores the yield was found to depend approximately linearly on the photon flux for low laser-pulse energies, whereas it saturates at higher energies. In Fig. 4 *A* the yield of pCA^- is shown at 430 nm, and the yield of pCT^- is shown in Fig. 4 *B* at 449 nm. These wavelengths are close to the respective absorption maxima where saturation is most likely. The yield is plotted as a function of the laser-pulse energy. The solid curve shows a fit to the data of the form $Y(\lambda) = a(1 - e^{-bE_{pulse}})$, where E_{pulse} is the averaged laser-pulse energy, and a and b are fitting parameters. The dashed curve is the corresponding linear approximation using the fitted values of a and b. The typical pulse energy during the measurement of the absorption profile is 0.2 mJ, which is within the linear range. Thus we further normalize the yield to the photon flux, which is proportional to $E_{pulse} \times \lambda$. The resulting formula for the relative absorption cross section is the following:

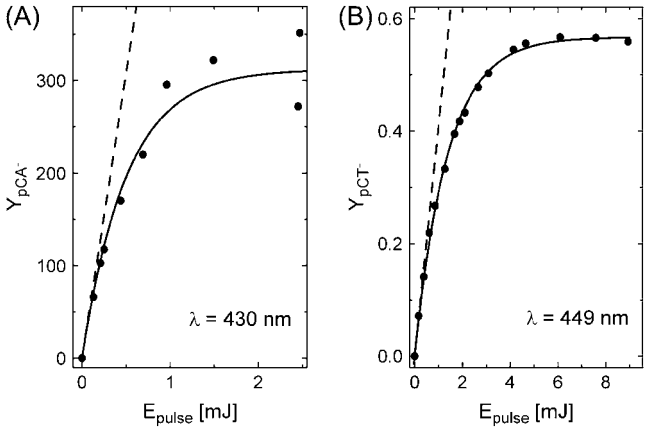

FIGURE 4 Yield of fragmentation as defined in the text is shown as a function of the average laser-pulse energy for the two model chromophores pCA^- (*A*) and pCT^- (*B*). The solid line is a fit to the data, and the dashed line is the corresponding linear approximation.

$$\sigma_{abs}(\lambda) \propto \frac{Y(\lambda)}{E_{pulse} \times \lambda}. \quad (3)$$

Here we assume that the quantum yield for photofragmentation is wavelength-independent, that the pulse energy is sufficiently low to avoid saturation, and that the overlap area between the ion bunch and the laser pulse remains constant during the measurement of the absorption profile.

RESULTS AND DISCUSSION

The absorption spectra of the two model chromophores in vacuum are shown in Fig. 5, *A* and *C*. The absorption maximum of the isolated pCA^- is around 430 nm with a full width at half-maximum of 25 nm. For pCT^- the absorption maximum is at 460 nm with a full width at half-maximum of 51 nm. The difference between the two chromophores consists of the thioester group being attached, and the negative charge being located primarily on the phenolate oxygen instead of the carboxylic oxygen. pCA^- is probably a better model for a neutral protein chromophore than for an anionic chromophore, since the phenol is not deprotonated, and the charge is not delocalized beyond the carboxylate group. Therefore a comparison between the two model chromophores in vacuum will give the sum of the effects from deprotonation of the phenol and formation of the thioester bond. In the gas phase this sum amounts to a significant red shift of 30 nm corresponding to 0.19 eV (Fig. 5, *A* and *C*).

In Fig. 5, *B* and *D*, the absorption spectra in water are seen. (See also Changenet-Barret et al. (15,16)). First we investigate the effect of deprotonation by comparing the dashed (neutral pH) and solid (alkaline pH) curves for each model chromophore. For pCA the maximum absorption in the

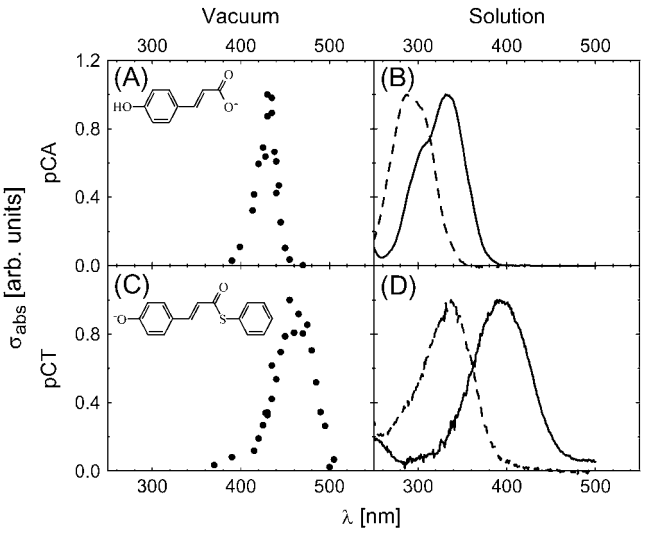

FIGURE 5 Absorption curves of the two model chromophores. (*A*) pCA^- in vacuum. (*B*) pCA in aqueous solution. The dashed line is for a neutral solution, and the solid line is for a solution with NaOH added, pH >11. (*C*) pCT^- in vacuum. (*D*) pCT in aqueous solution. The dashed line is for a neutral solution, and the solid line is for a borate (III) buffer, pH 10.2.

neutral aqueous solution is at 285 nm, with a shoulder at 312 nm. In the alkaline solution the absorption maximum is shifted to 336 nm, with a shoulder at ~300 nm. For pCT a similar red shift is observed from 337 nm at neutral pH to 395 nm at alkaline pH. The effect of thioester formation is then investigated by comparing the pCA^{2-} and the pCT^- chromophore. This effect amounts to a red shift from 336 nm to 395 nm.

Both deprotonation of the phenol and thioester formation thus have the effect of red-shifting the absorption of the chromophore in solution, with ~0.60 eV (4800 cm^{-1}) and ~0.55 eV (4400 cm^{-1}), respectively. This is in good agreement with previous studies (36) where the deprotonation was found to induce a shift of 4310 cm^{-1} (0.53 eV) when comparing the absorption of the denatured protein in neutral and alkaline pH. Similarly the shift induced by thioester formation was quantified by comparing the free coumaric acid and the denatured protein, both at neutral pH, giving a shift of 5712 cm^{-1} (0.71 eV).

The shift in the absorption maximum discussed above originates from changes directly on the chromophore. Apart from the effect of the intrinsic changes, the effect of the protein environment, i.e., the amino acids in the immediate vicinity of the chromophore, is interesting to investigate. The environmental effects have been studied by a couple of groups using site-specific mutagenesis (20–25). Several variants of PYP were made with mutations directed at the members of the hydrogen-bonding network that is thought to stabilize the negative charge on the chromophore: Tyr-42, Glu-46, and Thr-50. Also, mutations of the Arg-52 residue have been studied, since the positive group on the arginine residue was believed to stabilize the negative charge that is delocalized over the conjugated area. Mutants with neutral groups on this position did not shift the absorption maximum significantly though (447 nm for R52Q and 452 nm for R52A) (20,21). Therefore it was suggested that Arg-52 only plays a negligible role in the tuning of the absorption.

On the other hand, it was shown that the three members of the hydrogen-bonding network are definitely important for the fine-tuning of the absorption in PYP. Usually the hydrogen-bonding residues were exchanged by amino acids with lower or no possibility for hydrogen bonding. Upon interruption of the hydrogen-bonding network the absorption was shown to be red-shifted compared to wild-type PYP, except for one variant, E46D, which was 2 nm blue-shifted (22). The red shift was usually 10–15 nm (0.06–0.08 eV); the mutant with the largest shift was Y42F/E46Q, with an absorption maximum at 476 nm (25), corresponding to a shift of 0.18 eV from the wild-type protein.

The effect of hydrogen bonding in the chromophore environment has also been investigated using calculations by He et al. (26). They calculated the excitation energy of a phenolate anion in a protein environment modeled by a background charge distribution. This was compared to the excitation energy of the phenolate anion hydrogen-bonded to two water molecules at the Glu-46 and Tyr-42 positions in the same background charge environment. They found that the hydrogen bonds stabilize the ground state more than the excited state, leading to a blue shift of the excitation energy of 0.1269 eV. This result is in good agreement with the mutant studies described above.

The blue-shifting effect of the hydrogen-bonding network is, however, much smaller than the effect of solvation seen when the chromophores are dissolved in water. In aqueous solution, pCT^- has an absorption maximum at 395 nm, which is a blue shift of 0.46 eV relative to the gas-phase maximum at 460 nm (Fig. 6, *A* and *C*). This means that a complete solvation shell around the chromophore must have a large effect on the electronic states. A similar blue shift is seen for the denatured protein at pH 11, where the chromophore is deprotonated. Here the absorption maximum is at 398 nm (5). The denatured protein is only slightly less blue-shifted than the pCT^- model chromophore in solution. This probably means that the environment of the chromophore in the denatured protein is close to a regular aqueous solution, although the different nature of the two thioesters may also cause changes.

In the long-lived photocycle intermediate called pB or I_2 (6) the chromophore phenolate has been protonated and large conformational changes of the protein structure have taken place. Among these, the arginine 52 that protects the chromophore in the ground state (14) has moved substantially, thus exposing the chromophore to the solvent (10). Both protonation and solvent exposure are expected to induce blue shifts in the absorption spectrum, and indeed the absorption maximum of the pB state is blue-shifted to 355 nm (7) relative to the ground state of PYP at 446 nm. Although qualitatively in

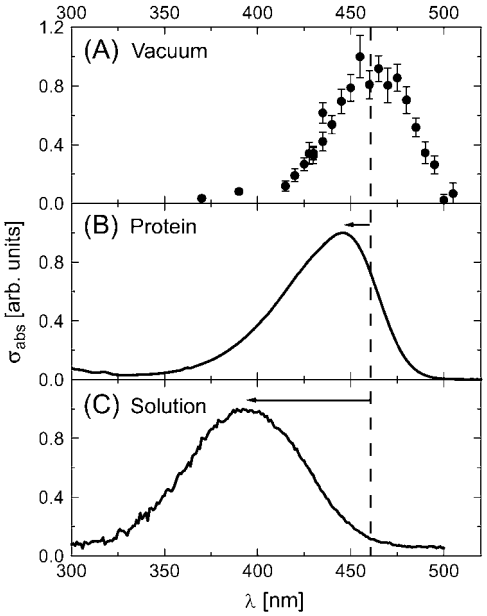

FIGURE 6 Absorption curves of the pCT^- chromophore in different environments. (*A*) pCT^- in vacuum ($\lambda_{max} = 460$ nm), (*B*) pCT^- in the protein ($\lambda_{max} = 446$ nm), and (*C*) pCT^- in alkaline aqueous solution ($\lambda_{max} = 395$ nm).

good agreement with the expectations, protonation and solvent exposure are of course not the only explanations for the blue shift since large changes in the protein structure have taken place that may further shift the absorption in either direction.

Of our two model chromophores, pCT^- is the best model for the PYP protein chromophore, so we will only be concerned with this model in the following discussion. There is only a rather small shift between the protein absorption and the absorption of the gas-phase pCT^- chromophore, as seen in Fig. 6, *A* and *B*. The protein environment blue-shifts the absorption from 460 nm to 446 nm, corresponding to 0.08 eV, but the blue shift is significantly smaller than the 0.46 eV shift observed in solution. For the PYP mutants where the hydrogen-bonding network is (partly) interrupted, the shift between the gas phase and the protein is even smaller. Thus the protein environment does not perturb the electronic states to the same degree as a complete solvation shell, or at least the ground and excited states are shifted by almost the same amount. It seems that in terms of electronic excitation the hydrophobic pocket where the chromophore is situated is better described by a vacuum than by an aqueous solution. The hydrogen bonds in the protein pocket (perhaps together with coulomb interactions) are hence important for fine-tuning the absorption maximum within ~20 nm, but the absorption of PYP is largely determined by the intrinsic properties of the chromophore.

These conclusions are consistent with previous findings on model chromophores of the green fluoerescent protein (37,38), a green fluorescent protein mutant (39), and the red fluorescent protein DsRed (40,41) in vacuum. The maximum absorption of the chromophore in vacuum is very close to the maximum absorption in the corresponding protein, whereas the absorption of the chromophore in solution is strongly blue-shifted. An explanation for this can be found in the secondary structure of the proteins (42–44). These proteins have a β-barrel structure with 11 β-strands surrounding the chromophore, and hence the proteins provide a very efficient shielding of the chromophore. Since a solvation shell cannot be created around the chromophore in the protein, the absorption is not blue-shifted as it is in solution. In the case of PYP the chromophore is also well protected from the solvent in the hydrophobic pocket.

Yoda et al. (30) have studied the deprotonated *trans*-thiopropyl-*p*-coumarate in 15 aprotic solvents of different dielectric constant and index of refraction. It was found that in high dielectric solvents like dimethylsulfoxide or dimethylformamide the absorption maximum (~456 nm) is very close to the gas-phase result for pCT^-, whereas for solvents of low polarity like pentane the absorption is shifted to ~368 nm. This is a surprising result since one would expect the gas phase to be the extreme case of low dielectric constant and index of refraction. Yoda et al. also conclude on the basis of the continuum model and regression analysis that the absorption maximum in the gas phase of their deprotonated propyl thioester is at 336 nm, far from the value we have measured. We have no explanation why the absorption in the gas phase can be similar to the absorption in high dielectric solvents, whereas in low dielectric solvents it is shifted, but the result illustrates that medium effects are by no means trivial.

The experimental absorption spectrum of the pCT^- chromophore can be compared with calculations. Molina and Merchán (27) have used ab initio calculations to study the deprotonated thiomethyl-*p*-coumarate in vacuum. They found that the first excited state of the *trans*-form is a $\pi\pi^*$-state lying 2.58 eV above the ground state, corresponding to $\lambda_{max} = 481$ nm. The only difference between this model and our pCT^- chromophore is the methyl group attached to the sulfur instead of the phenyl, which probably has only very small effects for the absorption maximum since the conjugated system does not extend beyond the sulfur. The result is in good agreement with our finding at 2.70 eV ($\lambda_{max} = 460$ nm).

Sergi et al. (28) used Car-Parrinello ab initio calculations based on density functional theory to study the anionic *trans*-thiophenyl-*p*-coumarate in vacuum. Their result for the energy of the first excited state is at 3.01 eV ($\lambda_{max} = 412.4$ nm), which is higher in energy than the measured 2.70 eV. They also performed a calculation where they took into account the effect of the protein environment on the chromophore. This was done by adding the hydrogen-bonding partners Glu-46, Tyr-42, and Thr-50, the counterion Arg-52, and the Cys-69 residues to the calculation. They find that the

absorption of the chromophore in the protein environment is slightly red-shifted to 2.97 eV ($\lambda_{max} = 417.6$ nm) compared to the vacuum calculation. The calculation including the protein environment hence also yields a higher excitation energy (2.97 eV) than the experimental value (2.78 eV). The calculation agrees well with our measurement in the sense that the shift between vacuum and the protein environment is small. The calculated shift, however, has a wrong sign.

The anionic *trans*-thiomethyl-*p*-coumarate in vacuum was also studied by Groenhof et al. (29) using molecular dynamics simulations and time-dependent density functional theory. Similar to the above calculation, their absorption maximum at 400 nm (3.10 eV) is higher in energy than the result of our measurement. On the other hand, when they include the protein environment in the calculation by adding the amino acid residues Cys-69, Arg-52, Thr-50, Glu-46, Tyr-42, and Phe-62, they end up at 442 nm (2.81 eV), close to the measured protein absorption maximum at 446 nm (2.78 eV). However, the significant red shift imposed by the protein environment in these calculations is in contradiction to our results. Because of the rather large discrepancies between the three calculations mentioned here it is clear that gas-phase absorption measurements are important for testing the accuracy of different types of calculations.

CONCLUSION

We have measured the absorption spectrum in vacuum of two PYP model chromophores. The maximum absorption of the deprotonated *trans*-*p*-coumaric acid is at 430 nm, whereas for the deprotonated *trans*-thiophenyl-*p*-coumarate it is at 460 nm. In aqueous solution the maximum absorption is at 336 nm and 395 nm, respectively.

The absorption spectrum of the deprotonated *trans*-thiophenyl-*p*-coumarate in vacuum is compared to that of the photoactive yellow protein. It is found that the protein absorption maximum is only blue-shifted 0.08 eV relative to that of the isolated chromophore. On the other hand, in aqueous solution solvation induces a large blue shift of the absorption maximum corresponding to 0.46 eV. This difference indicates that the absorption of the photoactive yellow protein is largely determined by the chromophore itself, but fine-tuning may be achieved by the protein environment through hydrogen bonds, charge distributions, and geometrical constraints. The protein environment is important, though, in the sense that it protects the chromophore from the surrounding solvent; in its absence the absorption would be significantly blue-shifted.

Ludovic Jullien, Pascale Changenet-Barret, and Monique Martin, Ecole Normale Supérieure, Paris, are thanked for providing the *trans*-thiophenyl-*p*-coumarate chromophore. Ulrich K. Genick, of The Scripps Research Institute, San Diego, CA, is thanked for providing the protein absorption curve.

This work was supported by the Danish Research Agency (contract 21-03-0330), the Danish Foundation for Basic Research, and the European Community's Research Training Program (contract HPRN-CT-2000-0142, ETR).

REFERENCES

1. Sprenger, W. W., W. D. Hoff, J. P. Armitage, and K. J. Hellingwerf. 1993. The eubacterium *Ectothiorhodospira halophila* is negatively phototactic, with a wavelength dependence that fits the absorption spectrum of the photoactive yellow protein. *J. Bacteriol.* 175:3096–3104.
2. van der Horst, M. A., and K. J. Hellingwerf. 2004. Photoreceptor proteins, ''Star actors of modern times'': a review of the functional dynamics in the structure of representative members of six different photoreceptor families. *Acc. Chem. Res.* 37:13–20.
3. Meyer, T. E. 1985. Isolation and characterization of soluble cytochromes, ferredoxins and other chromophoric proteins from the halophilic phototrophic bacterium *Ectothiorhodospira halophila*. *Biochim. Biophys. Acta.* 806:175–183.
4. Hoff, W. D., P. Düx, K. Hård, B. Devreese, I. M. Nugteren-Roodzant, W. Crielaard, R. Boelens, R. Kaptein, J. van Beeumen, and K. J. Hellingwerf. 1994. Thiol ester-linked *p*-coumaric acid as a new photoactive prosthetic group in a protein with rhodopsin-like photochemistry. *Biochemistry.* 33:13959–13962.
5. Baca, M., G. E. O. Borgstahl, M. Boissinot, P. M. Burke, D. R. Williams, K. A. Slater, and E. D. Getzoff. 1994. Complete chemical structure of photoactive yellow protein: Novel thioester-linked 4-hydroxycinnamyl chromophore and photocycle chemistry. *Biochemistry.* 33:14370–14377.
6. Meyer, T. E., E. Yakali, M. A. Cusanovich, and G. Tollin. 1987. Properties of a water-soluble, yellow protein isolated from a halophilic phototrophic bacterium that has photochemical activity analogous to sensory rhodopsin. *Biochemistry.* 26:418–423.
7. Hoff, W. D., I. H. van Stokkum, H. J. van Ramesdonk, M. E. van Brederode, A. M. Brouwer, J. C. Fitch, T. E. Meyer, R. van Grondelle, and K. J. Hellingwerf. 1994. Measurement and global analysis of the absorbance changes in the photocycle of the photoactive yellow protein from *Ectothiorhodospira halophila*. *Biophys. J.* 67:1691–1705.
8. Kort, R., H. Vonk, X. Xu, W. D. Hoff, W. Crielaard, and K. J. Hellingwerf. 1996. Evidence for *trans-cis* isomerization of the *p*-coumaric acid chromophore as the photochemical basis of the photocycle of photoactive yellow protein. *FEBS Lett.* 382:73–78.
9. Xie, A., W. D. Hoff, A. R. Kroon, and K. J. Hellingwerf. 1996. Glu46 donates a proton to the 4-hydroxycinnamate anion chromophore during the photocycle of photoactive yellow protein. *Biochemistry.* 35:14671–14678.
10. Genick, U. K., G. E. O. Borgstahl, K. Ng, Z. Ren, C. Pradervand, P. M. Burke, V. Šrajer, T.-Y. Teng, W. Schildkamp, D. E. McRee, K. Moffat, and E. D. Getzoff. 1997. Structure of a protein photocycle intermediate by millisecond time-resolved crystallography. *Science.* 275:1471–1475.
11. van Brederode, M. E., W. D. Hoff, I. H. M. van Stokkum, M. L. Groot, and K. J. Hellingwerf. 1996. Protein folding thermodynamics applied to the photocycle of the photoactive yellow protein. *Biophys. J.* 71: 365–380.
12. Genick, U. K., S. M. Soltis, P. Kuhn, I. L. Canestrelli, and E. D. Getzoff. 1998. Structure at 0.85 Å resolution of an early protein photocycle intermediate. *Nature.* 392:206–209.
13. Perman, B., V. Šrajer, Z. Ren, T. Teng, C. Pradervand, T. Ursby, D. Bourgeois, F. Schotte, M. Wulff, R. Kort, K. Hellingwerf, and K. Moffat. 1998. Energy transduction on the nanosecond time scale: Early structural events in a xanthopsin photocycle. *Science.* 279:1946–1950.
14. Borgstahl, G. E. O., D. R. Williams, and E. D. Getzoff. 1995. 1.4 Å structure of photoactive yellow protein, a cytosolic photoreceptor: Unusual fold, active site, and chromophore. *Biochemistry.* 34:6278–6287.
15. Changenet-Barret, P., P. Plaza, and M. M. Martin. 2001. Primary events in the photoactive yellow protein chromophore in solution. *Chem. Phys. Lett.* 336:439–444.
16. Changenet-Barret, P., A. Espagne, N. Katsonis, S. Charier, J.-B. Baudin, L. Jullien, P. Plaza, and M. M. Martin. 2002. Excited-state

relaxation dynamics of a pyp chromophore model in solution: influence of the thioester group. *Chem. Phys. Lett.* 365:285–291.

17. Larsen, D. S., M. Vengris, I. H. M. van Stokkum, M. A. van der Horst, R. A. Cordfunke, K. J. Hellingwerf, and R. van Grondelle. 2003. Initial photo-induced dynamics of the photoactive yellow protein chromophore in solution. *Chem. Phys. Lett.* 369:563–569.
18. Larsen, D. S., M. Vengris, I. H. M. van Stokkum, M. A. van der Horst, F. L. de Weerd, K. J. Hellingwerf, and R. van Grondelle. 2004. Photoisomerization and photoionization of the photoactive yellow protein chromophore in solution. *Biophys. J.* 86:2538–2550.
19. Ryan, W. L., D. J. Gordon, and D. H. Levy. 2002. Gas-phase photochemistry of the photoactive yellow protein chromophore *trans-p*-coumaric acid. *J. Am. Chem. Soc.* 124:6194–6201.
20. Genick, U. K., S. Devanathan, T. E. Meyer, I. L. Canestrelli, E. Williams, M. A. Cusanovich, G. Tollin, and E. D. Getzoff. 1997b. Active site mutants implicate key residues for control of color and light cycle kinetics of photoactive yellow protein. *Biochemistry.* 36:8–14.
21. Mihara, K., O. Hisatomi, Y. Imamoto, M. Kataoka, and F. Tokunaga. 1997. Functional expression and site-directed mutagenesis of photoactive yellow protein. *J. Biochem.* (*Tokyo*). 121:876–880.
22. Devanathan, S., R. Brudler, B. Hessling, T. T. Woo, K. Gerwert, E. D. Getzoff, M. A. Cusanovich, and G. Tollin. 1999. Dual photoactive species in Glu46Asp and Glu46Ala mutants of photoactive yellow protein: A pH-driven color transition. *Biochemistry.* 38:13766–13772.
23. Brudler, R., T. E. Meyer, U. K. Genick, S. Devanathan, T. T. Woo, D. P. Millar, K. Gerwert, M. A. Cusanovich, G. Tollin, and E. D. Getzoff. 2000. Coupling of hydrogen bonding to chromophore conformation and function in photoactive yellow protein. *Biochemistry.* 39:13478–13486.
24. Imamoto, Y., H. Koshimizu, K. Mihara, O. Hisatomi, T. Mizukami, K. Tsujimoto, M. Kataoka, and F. Tokunaga. 2001. Roles of amino acid residues near the chromophore of photoactive yellow protein. *Biochemistry.* 40:4679–4685.
25. Meyer, T. E., S. Devanathan, T. Woo, E. D. Getzoff, G. Tollin, and M. A. Cusanovich. 2003. Site-specific mutations provide new insights into the origin of pH effects and alternative spectral forms in the photoactive yellow protein from *Halorhodospira halophila*. *Biochemistry.* 42:3319–3325.
26. He, Z., C. H. Martin, R. Birge, and K. F. Freed. 2000. Theoretical studies on excited states of a phenolate anion in the environment of photoactive yellow protein. *J. Phys. Chem. A.* 104:2939–2952.
27. Molina, V., and M. Merchán. 2001. On the absorbance changes in the photocycle of the photoactive yellow protein: a quantum chemical analysis. *Proc. Natl. Acad. Sci. USA.* 98:4299–4304.
28. Sergi, A., M. Grüning, M. Ferrario, and F. Buda. 2001. Density functional study of the photoactive yellow protein's chromophore. *J. Phys. Chem. B.* 105:4386–4391.
29. Groenhof, G., M. F. Lensink, H. J. C. Berendsen, J. G. Snijders, and A. E. Mark. 2002. Signal transduction in the photoactive yellow protein. I. Photon absorption and the isomerization of the chromophore. *Proteins.* 48:202–211.
30. Yoda, M., H. Houjou, Y. Inoue, and M. Sakurai. 2001. Spectral tuning of photoactive yellow protein. Theoretical and experimental analysis of medium effects on the absorption spectrum of the chromophore. *J. Phys. Chem. B.* 105:9887–9895.
31. Møller, S. P. 1997. Elisa, an electrostatic storage ring for atomic physics. *Nucl. Instrum. Meth. Phys. Res. A.* 394:281–286.
32. Andersen, L. H., O. Heber, and D. Zajfman. 2004. Physics with electrostatic rings and traps. *J. Phys. B.* 37:R57–R88.
33. Andersen, J. U., E. Bonderup, and K. Hansen. 2001. On the concept of temperature for a small isolated system. *J. Chem. Phys.* 114:6518–6525.
34. Andersen, L. H., H. Bluhme, S. Boyé, T. J. D. Jørgensen, H. Krogh, I. B. Nielsen, S. B. Nielsen, and A. Svendsen. 2004. Experimental studies of the photophysics of gas-phase fluorescent protein chromophores. *Phys. Chem. Chem. Phys.* 6:2617–2627.
35. Andersen, J. U., P. Hvelplund, S. B. Nielsen, S. Tomita, H. Wahlgreen, S. P. Møller, U. V. Pedersen, J. S. Forster, and T. J. D. Jørgensen. 2002. The combination of an electrospray ion source and an electrostatic storage ring for lifetime and spectroscopy experiments on biomolecules. *Rev. Sci. Instrum.* 73:1284–1287.
36. Kroon, A. R., W. D. Hoff, H. P. M. Fennema, J. Gijzen, G.-J. Koomen, J. W. Verhoeven, W. Crielaard, and K. J. Hellingwerf. 1996. Spectral tuning, fluorescence, and photoactivity in hybrids of photoactive yellow protein, reconstituted with native or modified chromophores. *J. Biol. Chem.* 271:31949–31956.
37. Nielsen, S. B., A. Lapierre, J. U. Andersen, U. V. Pedersen, S. Tomita, and L. H. Andersen. 2001. Absorption spectrum of the green fluorescent protein chromophore anion in vacuo. *Phys. Rev. Lett.* 87: 228102.
38. Andersen, L. H., A. Lapierre, S. B. Nielsen, I. B. Nielsen, S. U. Pedersen, U. V. Pedersen, and S. Tomita. 2002. Chromophores of the green fluorescent protein studied in the gas phase. *Eur. Phys. J. D.* 20:597–600.
39. Boyé, S., I. B. Nielsen, S. B. Nielsen, H. Krogh, A. Lapierre, H. B. Pedersen, S. U. Pedersen, U. V. Pedersen, and L. H. Andersen. 2003. Gas-phase absorption properties of a green fluorescent protein-mutant chromophore: The w7 clone. *J. Chem. Phys.* 119:338–345.
40. Boyé, S., S. B. Nielsen, H. Krogh, I. B. Nielsen, U. V. Pedersen, A. F. Bell, X. He, P. J. Tonge, and L. H. Andersen. 2003. Gas-phase absorption properties of dsred model chromophores. *Phys. Chem. Chem. Phys.* 5:3021–3026.
41. Boyé, S., H. Krogh, I. B. Nielsen, S. B. Nielsen, S. U. Pedersen, U. V. Pedersen, L. H. Andersen, A. F. Bell, X. He, and P. J. Tonge. 2003. Vibrationally resolved photoabsorption spectroscopy of red fluorescent protein chromophore anions. *Phys. Rev. Lett.* 90:118103.
42. Ormö, M., A. B. Cubitt, K. Kallio, L. A. Gross, R. Y. Tsien, and S. J. Remington. 1996. Crystal structure of the *Aequorea victoria* green fluorescent protein. *Science.* 273:1392–1395.
43. Yang, F., L. G. Moss, and G. N. Phillips, Jr. 1996. The molecular structure of green fluorescent protein. *Nat. Biotechnol.* 14:1246–1251.
44. Wall, M. A., M. Socolich, and R. Ranganathan. 2000. The structural basis for red fluorescence in the tetrameric gfp homolog dsred. *Nat. Struct. Biol.* 7:1133–1138.